

Helicity separation in Heavy-Ion Collisions

Mircea Baznat,^{1,2,*} Konstantin Gudima,^{1,2,†} Alexander Sorin,^{1,3,‡} and Oleg Teryaev^{1,3,§}

¹*Joint Institute for Nuclear Research, 141980 Dubna (Moscow region), Russia*

²*Institute of Applied Physics, Academy of Sciences of Moldova, MD-2028 Kishinev, Moldova*

³*Dubna International University, Dubna (Moscow region) 141980, Russia*

(Dated: February 7, 2022)

We study the P-odd effects related to the vorticity of the medium formed in noncentral heavy ion collisions. Using the kinetic Quark-Gluon Strings Model we perform the numerical simulations of the vorticity and hydrodynamical helicity for the various atomic numbers, energies and centralities. We observed the vortical structures typically occupying the relatively small fraction of the fireball volume. In the course of numerical simulations the noticeable hydrodynamical helicity was observed manifesting the specific mirror behaviour with respect to the reaction plane. The effect is maximal at the NICA and FAIR energy range.

PACS numbers: 25.75.-q

I. INTRODUCTION

The local violation [1] of discrete symmetries in strongly interacting QCD matter is now under intensive theoretical and experimental investigations. The renowned Chiral Magnetic Effect (CME) uses the (C)P-violating (electro)magnetic field emerging in heavy ion collisions in order to probe the (C)P-odd effects in QCD matter.

There is an interesting counterpart of this effect, Chiral Vortical Effect (CVE)[2] due to coupling to P-odd medium vorticity. In its original form [2] this effect leads to the appearance of the same electromagnetic current as CME. Its straightforward generalization was proposed later resulting in generation of all conserved-charge currents [3], in particular baryonic ones (especially important when there is CME cancellation between three massless flavors [4]), and polarization of hyperons [3, 5]. Let us also mention quite recent very interesting theoretical development [6], where a remarkable relation to the gravitational anomalies was discovered.

The key problem is whether the flows developing in heavy ion collisions indeed possess the vorticity?! This is especially interesting as vorticity is universal phenomenon manifested at very different scales of macro and micro physics. One can observe it in spiral galaxies, cyclones and typhoons, semiconductors, chemical reactions, biological systems, quantum field theories, etc. It would be indeed very important to push this concept further to the internal structure of QCD matter.

The noncentral heavy ion collisions could naturally generate a rotation (global or local, both related to vorticity) with an angular velocity normal to the reaction plane, which is their generic qualitative feature. However finding proper quantitative characteristics of these phenomena requires special investigation [7, 8]. In this paper we address this problem using the Quark-Gluon Strings Model (QGSM) and observe the clear signs and manifestations of vortical and helical structures in QCD matter formed in noncentral heavy ion collisions. In particular we observed the novel effect of the hydrodynamical helicity separation.

II. MODELLING VELOCITY, VORTICITY AND HELICITY IN KINETIC MODEL

One of the first models designed to describe the dynamics of energetic heavy-ion collisions was the intra-nuclear cascade model developed in Dubna [9] which is based on the Monte-Carlo solution of a set of the Boltzmann-Uehling-Uhlenbeck relativistic kinetic equations with the collision terms, including cascade-cascade interactions. For particle energies below 1 GeV it is sufficient to consider only nucleons, pions and deltas. The model includes a proper description of pion and baryon dynamics for particle production and absorption processes. In the original version the nuclear potential is treated dynamically, i.e., for the initial state it is determined using the Thomas-Fermi approximation,

*Electronic address: baznat@theor.jinr.ru

†Electronic address: gudima@theor.jinr.ru

‡Electronic address: sorin@theor.jinr.ru

§Electronic address: teryaev@theor.jinr.ru

but later on its depth is changed according to the number of knocked-out nucleons. This allows one to account for nuclear binding. The Pauli principle is implemented by introducing a Fermi distribution of nucleon momenta as well as a Pauli blocking factors for scattered nucleons.

At energies higher than about 10 GeV, the Quark-Gluon String Model (QGSM) is used to describe elementary hadron collisions [10, 11]. This model is based on the $1/N_c$ expansion of the amplitude for binary processes where N_c is the number of quark colours. Different terms of the $1/N_c$ expansion correspond to different diagrams which are classified according to their topological properties. Every diagram defines how many strings are created in a hadronic collision and which quark-antiquark or quark-diquark pairs form these strings. The relative contributions of different diagrams can be estimated within Regge theory, and all QGSM parameters for hadron-hadron collisions were fixed from the analysis of experimental data. The break-up of strings via creation of quark-antiquark and diquark-antidiquark pairs is described by the Field-Feynman method [12], using phenomenological functions for the fragmentation of quarks, antiquarks and diquarks into hadrons. The modified non-Markovian relativistic kinetic equation, having a structure close to the Boltzmann-Uehling-Uhlenbeck kinetic equation, but accounting for the finite formation time of newly created hadrons, is used for simulations of relativistic nuclear collisions. One should note that QGSM considers the two lowest SU(3) multiplets in mesonic, baryonic and antibaryonic sectors, so interactions between almost 70 hadron species are treated on the same footing. This is a great advantage of this approach which is important for the proper evaluation of the hadron abundances and characteristics of the excited residual nuclei. The energy extremes were bridged by the QGSM extension downward in the beam energy [13].

For investigation of dynamical formation of velocity \vec{v} and vorticity $\vec{\omega} (\equiv \text{rot } \vec{v})$ fields in relativistic heavy ion collision the coordinate space was divided into $50 \times 50 \times 100$ cells of volume $dxdydz$ with $dx = dy = 0.6 \text{ fm}$, $dz = 0.6/\gamma \text{ fm}$, where γ is the gamma factor of equal velocity system of collision. In this reference system the total momentum and total energy of the produced particles were calculated in all cells for each of fixed 25 moments of time t covering the interval of $10 \text{ fm}/c$.

The results were averaged for about 10000 heavy ion collisions with identical initial conditions. The spectator nucleons of projectile or target ions, which at given time momentum do not undergone any individual collision, were included in evaluation of velocity. The velocity field in the given cell was defined by the following double sum over the particles in the cell and over the all simulated collisions:

$$\vec{v}(x, y, z, t) = \frac{\sum_i \sum_j \vec{P}_{ij}}{\sum_i \sum_j E_{ij}} \quad (1)$$

where \vec{P}_{ij} and E_{ij} are the momentum and energy of particle i in the collision j , respectively. The vorticity was calculated using the discrete partial derivatives.

We paid a special attention to the pseudoscalar characteristics of the vorticity, that is the hydrodynamical helicity $H \equiv \int dV (\vec{v} \cdot \vec{\omega})$ which is related to a number of interesting phenomena in hydrodynamics and plasma physics, such as

the turbulent dynamo and Lagrangian chaos. It might be compared the analog of topological charge $Q = \int d^3x J^0(x)$

where the current $J^\mu = \epsilon^{\mu\nu\rho\gamma} u_\nu \partial_\rho u_\gamma$ (as usual, the four-velocity $u_\nu \equiv \gamma(1, \vec{v})$) contributes to the hydrodynamical anomaly [14] and the polarization of hyperons [3, 5]. The calculation of the topological charge which is the correct relativistic generalization of the hydrodynamical helicity leads to the extra factor γ^2 in the integrand. Still as the helicity itself is a more traditional quantity, we use it for the numerical calculations.

III. RESULTS OF THE SIMULATIONS: HELICITY SEPARATION EFFECT

The qualitative pictures of velocity and vorticity fields corresponding to $Au + Au$ collisions at $\sqrt{s_{NN}} = 5 \text{ GeV}$ with the impact parameter 8 fm equal to the (transverse) radius of the nuclei are presented at figures 1-2.

Figure 1 represents the three dimensional distribution (top) of the velocity defined by the collision participants and produced particles after $10 \text{ fm}/c$ of the evolution, and its projection (bottom) to the transverse xy -plane. The direction, length and color of the arrows represent the direction and size of the velocity. We clearly see the picture of a little bang when fastest particles (pions) are occupy most distance positions from the collision origin.

Fig. 2 represents the similar distributions for the vorticity. The vorticity is concentrated in the relatively thin ($2 \div 3 \text{ fm}$) layer at the boundary of the participant region. This might be an analog of the vortex sheet expected when Kelvin-Helmholtz instability develops [15]. Let us stress that in the case under consideration it emerges in the kinetic approach which might be of some interest for the microscopic description of turbulence.

For quantitative description of this phenomena we, as it was already mentioned, use the hydrodynamic helicity whose patterns are presented on Figures 3-6.

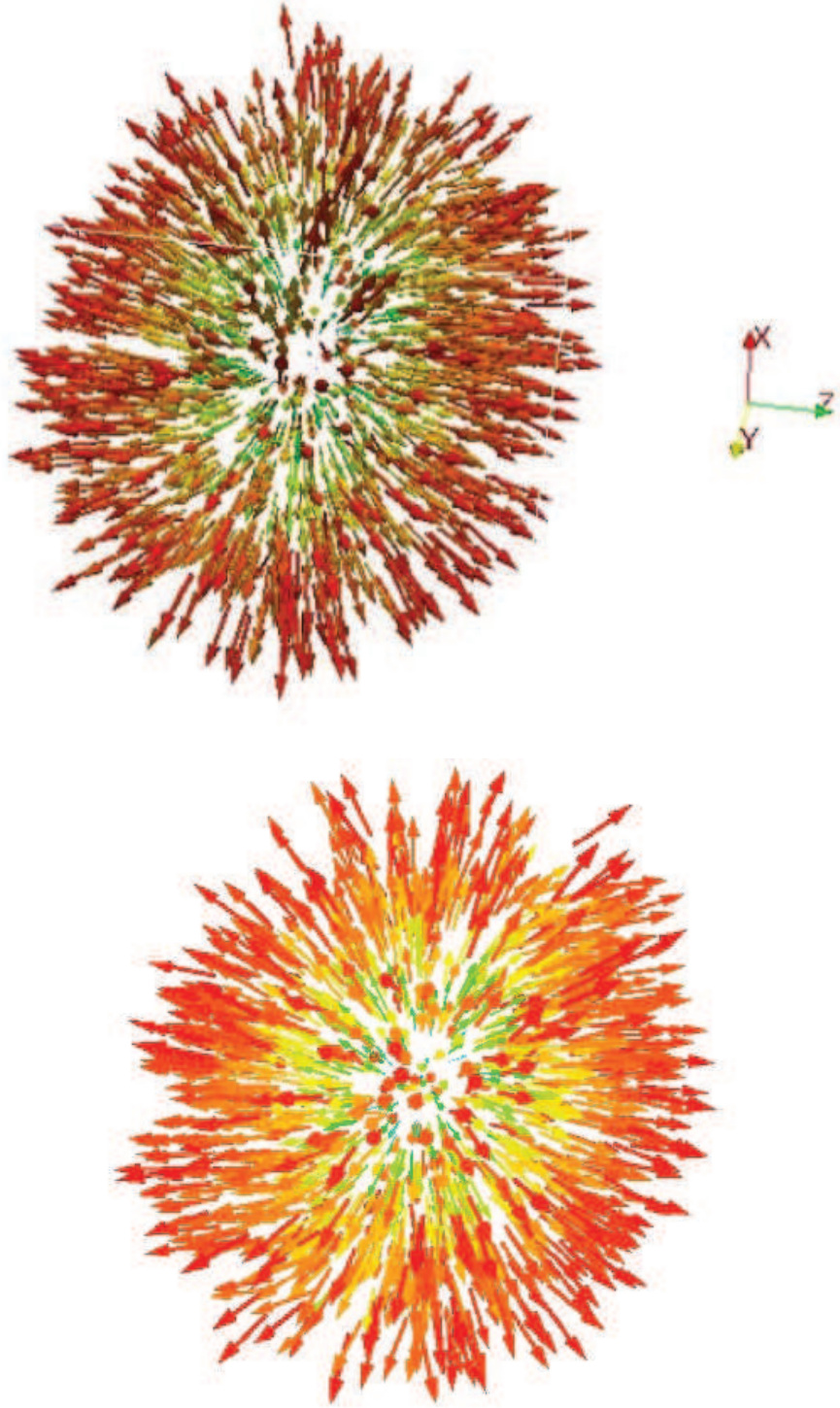


Figure 1: (color online) Three dimension image (top) and projection on plane XY (bottom) of velocity field in Au+Au at $\sqrt{s_{NN}} = 5 \text{ GeV}$, $b = 8 \text{ fm}$ and $t = 10 \text{ fm}/c$

Fig. 3 represents the helicities in gold-gold collisions at different impact parameters evaluated in different domains. One can see that the helicity calculated with inclusion of the all cells is zero (black line). For the cells with the definite sign of the velocity components, which are orthogonal to the reaction plane (which may be selected also experimentally), the helicity is nonzero and changes the sign for the different signs of these components (red and blue

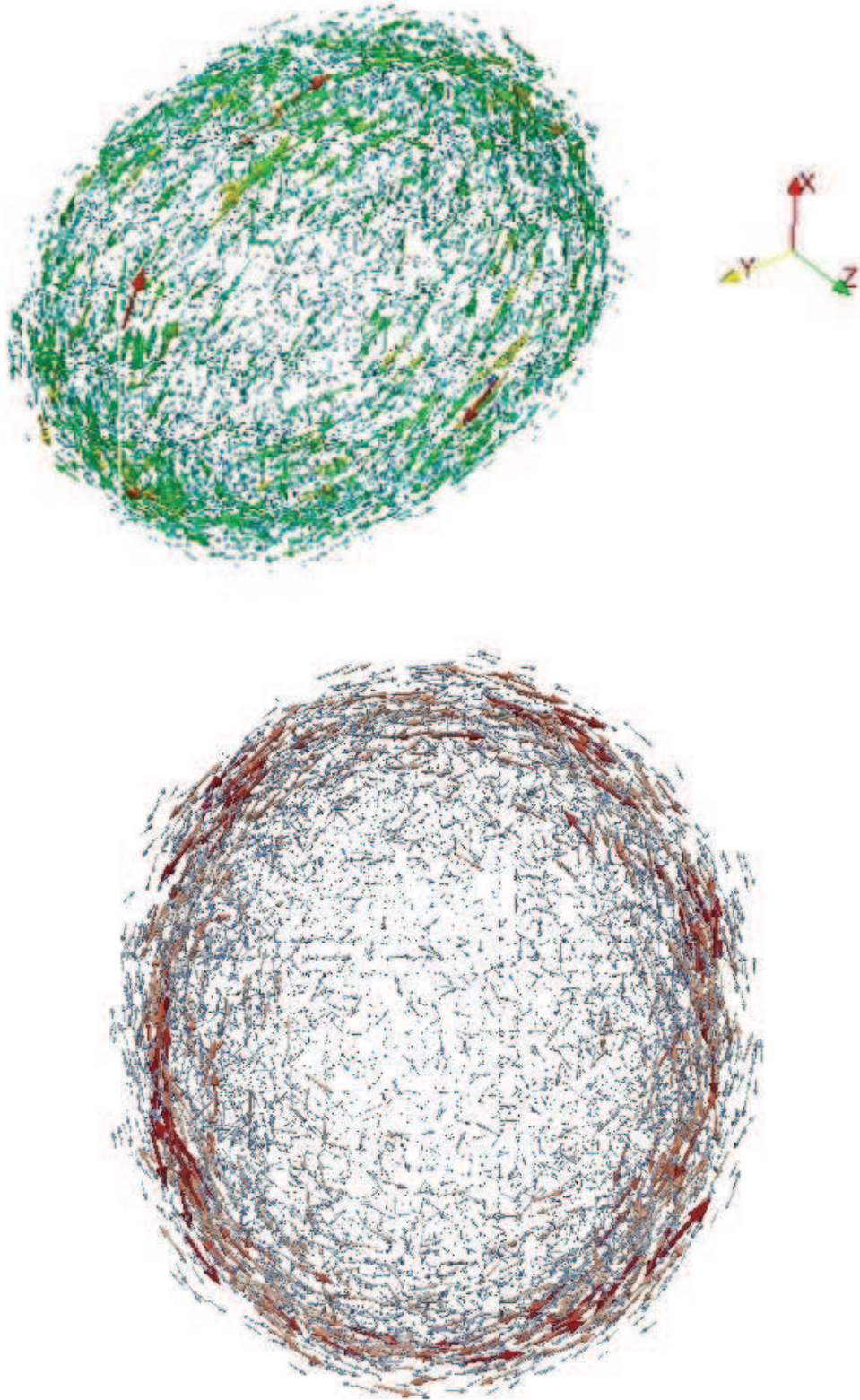


Figure 2: (color online) Three dimension image (top) and projection on plane XY (bottom) of vorticity field in Au+Au at $\sqrt{s_{NN}} = 5 \text{ GeV}$, $b = 8 \text{ fm}$ and $t = 10 \text{ fm}/c$

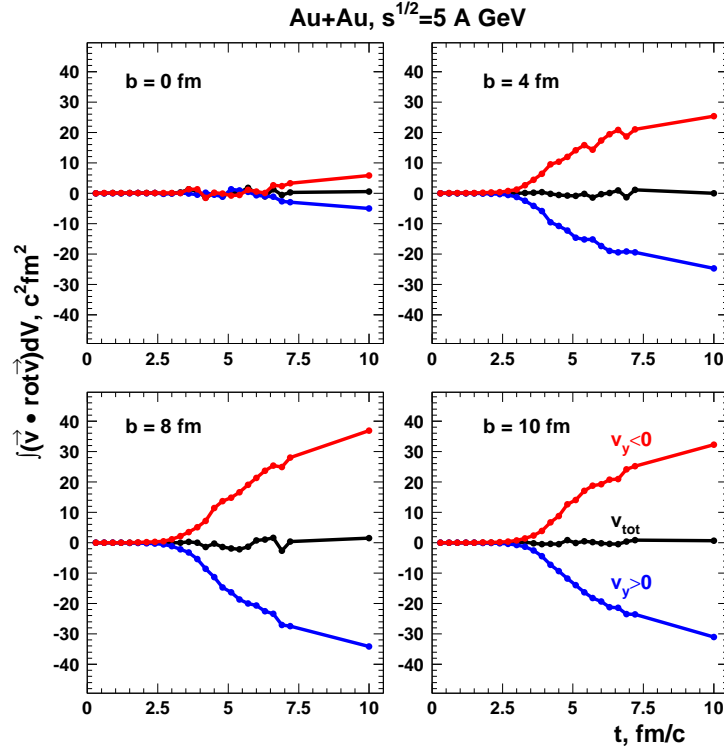


Figure 3: (color online) Time dependence of helicity at different impact parameters

lines, respectively). The effect is growing with impact parameter and represents a sort of saturation in time. This

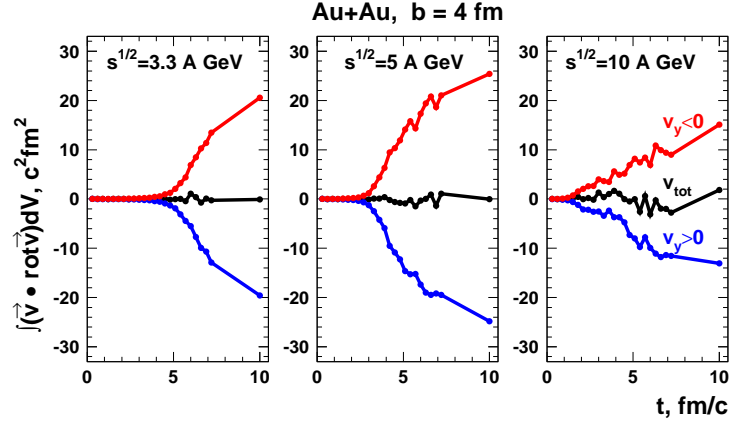


Figure 4: (color online) Time dependence of helicity at different energies

effect of helicity separation is one of our main results. Let us stress that the calculation in the hybrid UrQMD model manifests very similar behavior [16]. This is not surprising as the helicity is in fact generated at the hydrodynamical stage of the model, while the transition from kinetic to hydrodynamical stage should be performed similarly to our Eq. (1).

This effect might be qualitatively explained, if the perpendicular components of velocities (which are selected to have different signs) and the corresponding vorticities (assumed to have the same signs) provide the dominant contribution to the scalar product in the helicity definition. However, the numerical analysis showed that the longitudinal

components along the beam directions (z-axis) provide even larger contribution to the helicity than contributions from the transverse direction (y-axis). So, such qualitative picture is oversimplified, but still provides a correct sign convention for the helicity-separation effect.

Fig. 4 represents the energy dependence of helicity which shows that its maximal value is achieved around the NICA energy range.

Fig. 5 shows how the effect is manifested in asymmetric collisions of gold and argon ions in comparison to the gold-gold ones.

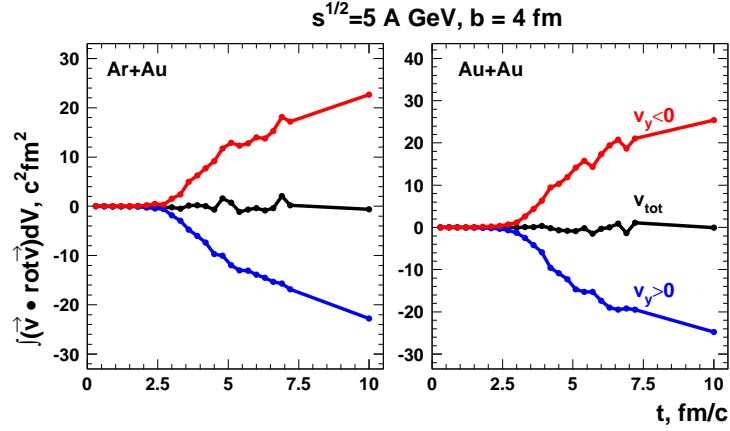


Figure 5: (color online) Time dependence of helicity in asymmetric collisions

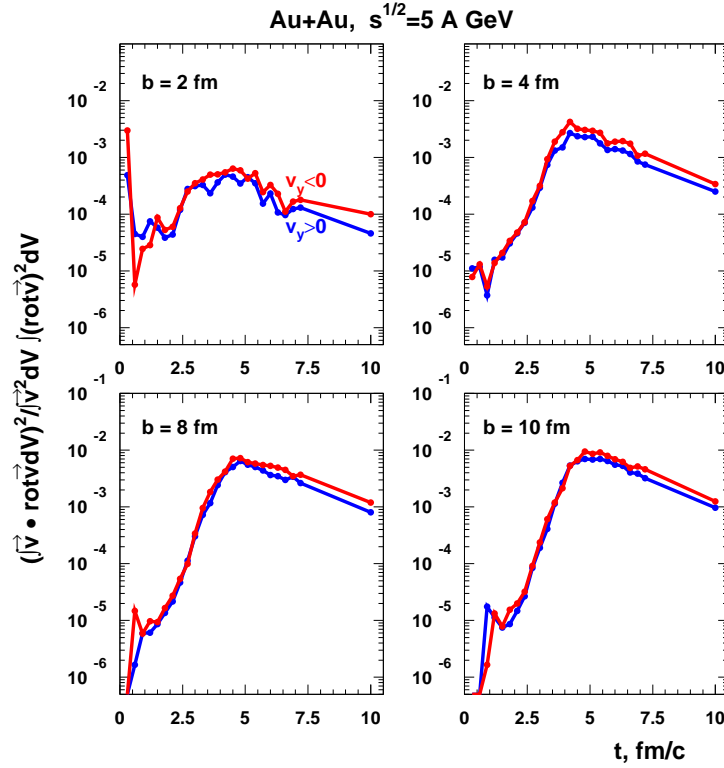


Figure 6: (color online) Time dependence of Cauchy-Schwarz bound for helicity

Fig. 6 shows the dimensionless ratio bounded from above by 1 due to Cauchy-Schwarz inequality. This bound is

saturated for helical flows with vorticities parallel to velocities. In the case of incompressible fluids the helicity of such flows is proportional to the (non-relativistic) kinetic energy. The actual values of this ratio show that the correlation between the directions of the vorticity and the velocity is not large, but non-negligible.

IV. CONCLUSIONS

We investigated vorticity and hydrodynamical helicity in noncentral heavy-ion collisions in the framework of the kinetic quark-gluon string model. We have observed that the vorticity is predominantly localized in a relatively thin layer ($2 \div 3 fm$) on the boundary between the participant and spectator nucleons. This might be qualitatively understood in the spirit of the core-corona type models [17, 18]. Thus, the gradients of the velocities in the region occupied by the participants are small due to the compensation of momenta between the target and projectile particles in the c.m. frame. As the result the vorticity is substantial only in the thin transition layer between the participant (i.e., core) and the spectator (i.e., corona) regions. We found the novel effect of the helicity separation in heavy-ion collisions when it has the different signs below and above of the reaction plane. We have investigated its dependence on the type of nuclei and collision energy and observed that it is maximal in the NICA energy range. We have also calculated the degree of alignment of the velocity and vorticity which is maximal for the Beltrami flows whose relativistic generalization is currently under investigation [19].

Acknowledgements

We are indebted to E.L. Bratkovskaya, K.A. Bugaev, L. Csernai, V.D. Kekelidze, V.D. Toneev, V. Voronyuk, V.I. Zakharov, G.M. Zinovjev and, especially, M. Bleicher, J. Steinheimer and H. Stöcker for useful discussions and comments. This work was supported in part by the Russian Foundation for Basic Research, Grant No. 11-02-01538-a.

-
- [1] K. Fukushima, D.E. Kharzeev and H.J. Warringa, Phys. Rev. D **78**, 074033 (2008) [arXiv:0808.3382 [hep-ph]].
 - [2] D. Kharzeev and A. Zhitnitsky, Nucl. Phys. A **797**, 67 (2007) [arXiv:0706.1026 [hep-ph]].
 - [3] O. Rogachevsky, A. Sorin and O. Teryaev, Phys. Rev. C **82**, 054910 (2010) [arXiv:1006.1331 [hep-ph]].
 - [4] D. E. Kharzeev and D. T. Son, Phys. Rev. Lett. **106**, 062301 (2011) [arXiv:1010.0038 [hep-ph]].
 - [5] J. -H. Gao, Z. -T. Liang, S. Pu, Q. Wang and X. -N. Wang, Phys. Rev. Lett. **109**, 232301 (2012) [arXiv:1203.0725 [hep-ph]].
 - [6] K. Landsteiner, E. Megias, L. Melgar and F. Pena-Benitez, JHEP **1109** (2011) 121 [arXiv:1107.0368 [hep-th]].
 - [7] F. Becattini and L. Tinti, Annals Phys. **325**, 1566 (2010) [arXiv:0911.0864 [gr-qc]].
 - [8] B. Betz, M. Gyulassy and G. Torrieri, Phys. Rev. C **76**, 044901 (2007) [arXiv:0708.0035 [nucl-th]].
 - [9] V.D. Toneev, K.K. Gudima, Nucl. Phys. A **400**, 173c (1983).
 - [10] V.D. Toneev, N.S. Amelin, K.K. Gudima, S.Yu. Sivoklokov, Nucl. Phys. A **519**, 463c (1990).
 - [11] N.S. Amelin, E.F. Staubo, L.S. Csernai et al., Phys.Rev. C **44**, 1541 (1991).
 - [12] R.D. Field, R.P. Feynman, Nucl. Phys. B **136**, 1 (1978).
 - [13] N.S. Amelin, K.K. Gudima, S.Yu. Sivoklokov, V.D. Toneev, Sov. J. Nucl. Phys. **52**, 272 (1990).
 - [14] D.T. Son and P. Surowka, Phys. Rev. Lett. **103**, 191601 (2009) [arXiv:0906.5044 [hep-th]].
 - [15] L. P. Csernai, D. D. Strottman and C. .Anderlik, Phys. Rev. C **85** (2012) 054901 [arXiv:1112.4287 [nucl-th]].
 - [16] J. Steinheimer, private communication.
 - [17] J. Aichelin and K. Werner, aXiv:0810.4465[nucl-th]
 - [18] J. Steinheimer and M. Bleicher, arXiv:1104.3981[nucl-th]
 - [19] A.S. Sorin, O.V. Teryaev, work in progress.